fortune Journals

Research Article

FORTUNE JOURNAL OF HEALTH SCIENCES

ISSN: 2644-2906

Synthesis and Chemistry of Recombinant Gelsolin 1-3 as A Probe for The Ovarian Cancer Biomarker Lysophosphatidic Acid

Navina Lotay, Cynthia Maria Suarez, Brian De La Franier, Rebecca Ann Jockusch and Michael Thompson*

Abstract

Gelsolin is an actin-binding protein that is competitively bound by lysophosphatidic acid (LPA), a possible biomarker for the early detection of ovarian cancer. Our group has previously shown the usage of gelsolin 1-3 (a fragment of gelsolin composed of the first three of its six subdomains) along with actin to detect the presence of lysophosphatidic acid. This histidine-tagged gelsolin 1-3 fragment is synthesized in our lab using bl21 Rosetta cells but required further characterization. This study aims to provide sufficient characterization of gelsolin 1-3 synthesized in our lab via both sodium dodecyl sulfate polyacrylamide gel electrophoresis (SDS-PAGE) and mass spectrometry (MS) using a Fourier-transform ion cyclotron resonance mass spectrometer (FTICR-MS). These techniques show the presence of protein at the expected mass of approximately 41 kDa. Additionally, the dissociation of a smaller fragment of the complex when introduced into the gas phase which was equivalent to the approximate mass of one subdomain of gelsolin 1-3 further supports this conclusion.

Keywords: Gelsolin, SDS-PAGE, FTICR-MS, Mass spectrometry, Protein characterization

Introduction

Gelsolin is an 82 kDa calcium-dependent actin-binding protein that regulates cell motility and morphology through actin filament assembly and disassembly. Actin is a protein that forms microfilaments in the cell cytoskeleton and is therefore the most abundant protein in most eukaryotic cells [1]. Gelsolin binds actin monomers, severs actin filaments, and nucleates actin polymerization to form new filaments. For this to occur, actin can bind to gelsolin at three different sites [2]. The affinity for this binding is heavily dependent on the particular binding site and the presence and type of salts, with K_d measured to be as low as 4.5 pM and as high as 400 μM [3–5]. Gelsolin consists of six homologous domains, 1-6, each containing a five-stranded β-sheet flanked by two α-helices: one parallel to the strands and one perpendicular [6]. The subdomains form two identical complexes (domains 1-3 and 4-6) [7–9] (Figure 1).

Lysophosphatidic acid, a promising ovarian cancer biomarker, is a regulator of actin-gelsolin binding. It binds to the PIP_2-binding domain of gelsolin with a K_d of 6 nM, causing the release of actin [7,11]. Interestingly, each half of gelsolin can individually bind to LPA [7,11]. LPA has been found to have a sensitivity of 98% and specificity of 90% in the detection of ovarian cancer, with levels shown to increase with disease progression

Affiliation:

Department of Chemistry, University of Toronto, 80 St. George Street, Toronto ON M5S 3H6

***Corresponding author:**
Michael Thompson, Department of Chemistry, University of Toronto, 80 St. George Street, Toronto ON M5S 3H6, Canada.

Citation: Navina Lotay, Cynthia Maria Suarez, Brian De La Franier, Rebecca Ann Jockusch and Michael Thompson. Synthesis and Chemistry of Recombinant Gelsolin 1-3 as A Probe for The Ovarian Cancer Biomarker Lysophosphatidic Acid. Fortune Journal of Health Sciences. 7 (2024): 670-675.

Received: October 25, 2024
Accepted: November 01, 2024
Published: November 15, 2024

[12,13]. As the 5-year survival rate for ovarian cancer patients is approximately 90% when detected in Stage I but drops to approximately 30% when detected in Stage IV, early detection is critical to improving patient prognosis [14]. Current detection methods for LPA rely on standard analytical methods that employ expensive instrumentation and time-intensive sample preparation practices. As such, there is a need for detection methods that are rapid, low-cost, and usable in serum.

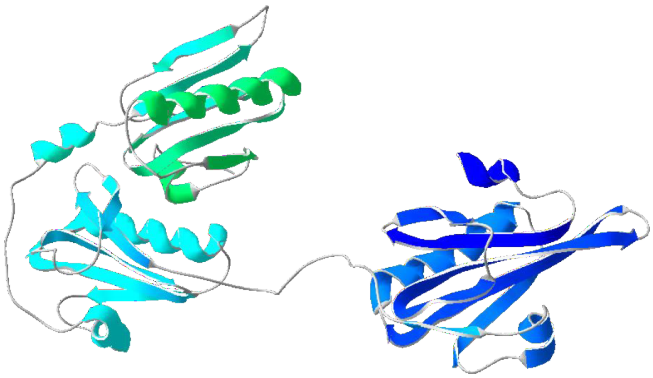

Figure 1: The crystal structure of gelsolin 1-3 obtained from the RCSB Protein Data Bank; PDB ID: 1RGI. http://doi.org/10.2210/pdb1rgi/pdb

Our group has previously shown the application of the interactions between gelsolin, actin, and lysophosphatidic acid in both a fluorescence-based optical biosensor and electrochemistry-based biosensor for the early detection of ovarian cancer [15,16]. We found that using one half of the full protein complex (gelsolin 1-3) works just as well, if not better than, using full-length gelsolin, while taking up less space on the biosensor surface. Currently, we are working on new biosensors taking advantage of this same system but with different detection methods such as chemiluminescence and electromagnetic piezoelectric acoustic sensors (EMPAS) [18]. This work aims to further confirm and characterize the recombinant gelsolin 1-3 synthesized and used for these biosensors intended for the early diagnosis of ovarian cancer through gel electrophoresis in combination with mass spectrometry (MS).

Polyacrylamide gel electrophoresis (PAGE) is a well-established technique commonly used to assess the size of proteins and other molecules. For this study, as done previously [3,5], denaturing gels were used to assess the size and molecular weight of the gelsolin 1-3 produced along with the purity of the samples from each step in the purification process. While PAGE gels for full-length gelsolin have been published previously, data for gelsolin 1-3 has not.

Gel electrophoresis on its own, however, is not enough to identify a protein – while it gives information on total mass, many proteins or other complexes can have the same mass; thus, complementary techniques must be employed. MS has become a valuable technique for this endeavor as it is a powerful analytical tool that gives detailed structural and identifying information about chemical compounds and complexes [18]. Initially, harsh ionization methods restricted gas-phase characterization to small, highly volatile organic analytes [19–22]. This would provide information about their amino acid composition while losing precious structural insights. It wasn't until the 1980s when the development of gentle ionization techniques allowed for the analysis of proteins and their complexes with little to no fragmentation [23, 24]. MS has been evidenced to be a great complementary technique to traditional tools for biomolecule analysis such as gel electrophoresis and antibody capture assays [25]. This work aims to use MS as a complementary technique to confirm the successful production of gelsolin 1-3 using Fourier transform ion cyclotron resonance MS (FTICR-MS). FTICR-MS is the ideal instrumentation for this purpose due to its high resolving power, mass accuracy, and ability to be coupled with versatile fragmentation techniques [18, 24]. While mass spectrometry has been performed on gelsolin isoforms previously [26,27], it has only been done on the peptides of trypsin-digested gelsolin; this work represents the first instance of the undigested protein gelsolin 1-3 being sprayed whole and analyzed with FTICR-MS. The results from both gel electrophoresis and MS confirm through mass and structural information the successful synthesis of recombinant gelsolin 1-3 which can continue to be used in the development of biosensors for LPA that could lead to the early detection of ovarian cancer.

Materials and Methods

Materials

Plasmids containing histidine-tagged gelsolin 1-3 were provided by Professor Robert C. Robinson of the University of Singapore. Lysogeny broth (LB), bl21 cells, DNase I (Thermo Scientific, EN-521), and Invitrogen™ BenchMark™ Prestained Protein Ladder (Invitrogen™, 10748010) were purchased from MedStore at the University of Toronto (Toronto, ON). All other chemicals and materials were purchased from Millipore Sigma (Oakville, ON), unless otherwise noted.

Expression and Synthesis of Gelsolin 1-3

Cell stocks of bl21 Rosetta cells containing the plasmid encoded with the DNA for histidine-tagged gelsolin 1-3 are stored at -30˚ C in 200 µL aliquots. To produce gelsolin 1-3, one aliquot of cells was thawed and grown in 30 mL of LB buffer (25 g/L LB, 100 mg/L ampicillin) at 37˚ C overnight. The solution was then diluted into 2 L of LB buffer and grown at 37˚ C until an optical density of 0.5 at 600 nm is achieved. At this point, protein production was induced

Lotay N., Fortune J Health Sci 2024
DOI:10.26502/fjhs.236

with the addition of isopropyl β-D-1-thiogalactopyranoside (IPTG) to obtain a final concentration of 1 mM. Protein production was allowed to continue overnight at room temperature. Cells were then pelleted by centrifugation for 20 minutes at 4800 RPM and then re-suspended in 4 mL of lysis buffer (20 mM imidazole, 20 mM Tris pH 7.2, 300 mM NaCl, 0.1% Triton-X, 5% glycerol, 1 mg/mL lysozyme, and 1 protease inhibitor tablet) and sonicated for 30 min. Then, 2 µL DNAse I was added to the suspension before rocking it gently for 30 min. The suspension was then centrifuged for 45 min at 14,500 RPM. Histidine-tagged gelsolin 1-3 was isolated from the supernatant using a Ni-NTA agarose affinity column and then concentrated and buffer exchanged using a 10k molecular weight cutoff (MWCO) Amicon® Ultra centrifugal filter (UFC5010) into storage buffer (20 mM HEPES pH 7.8, 3 mM $CaCl_2$).

SDS-PAGE

A separating gel (12% w/v acrylamide, 0.4 M TRIS pH 8.8, 0.1% SDS) was prepared and polymerized with 10% APS (60 µL), and tetramethylethylenediamine (TEMED, 10 µL). A stacking gel (4% w/w acrylamide, 0.4 M TRIS pH 6.8, 0.1% SDS) was prepared, polymerized with 10% w/v APS (30 µL) and TEMED (10 µL), and added on top of the separating gel with a comb to form the sample wells. Samples of 10 µL were taken from each step of the purification process of gelsolin 1-3. 2 µL of loading dye (0.1 M TRIS pH 8.8, 3.6% SDS, 27% glycerol, 0.02% w/v bromophenol blue, 1.8% β-mercaptoethanol) were added to each sample. These samples, along with 10 µL of protein ladder, were run on the gel at 120 V for 1 hour. The gel was stained by submerging it in Coomassie blue stain (40% methanol, 10% glacial acetic acid, 0.5% w/v Coomassie R-250) and incubating at 37˚ C for 30 minutes. It was then destained by submersion in strong destain (40% methanol, 10% glacial acetic acid) for 10 minutes followed by weak destain (10% methanol, 10% glacial acetic acid) for 30 minutes, both with gentle agitation of the sample at room temperature. The gel was imaged using the Syngene G:BOX (New England BioGroup, Atkinson, NH).

Mass Spectrometry

The HEPES buffer which the gelsolin 1-3 was stored in was removed using a 3K MWCO Amicon® ultra centrifugal filter (UFC5003). After three washes with 10 mM ammonium acetate, the desalted synthesized gelsolin 1-3 was diluted in 10 mM ammonium acetate to a concentration of 5 µM.

A 7T FT-ICR mass spectrometer (Bruker Apex Qe, Bruker Daltonics, Billerica, MA) was used for mass spectral characterization. Positive nano-electrospray ionization (nano-ESI) was used to spray gelsolin 1-3 out of borosilicate capillary tips (Sutter Instrument, o.d. 1.0 mm, i.d. 0.75 mm) pulled to a 2.5 µm opening using a micropipette puller (Model P97, Sutter Instrument, Novato, CA). A platinum wire was inserted into the capillary tip to serve as the grounded electrode, while the mass spectrometer inlet was operated at an 800V potential drop to act as the counter electrode. The ions passed through a heated capillary with counter drying nitrogen gas to aid desolvation as they entered the mass spectrometer. The pressure at the first pumping stage was raised to 4.50 mbar to aid with collisional cooling of ions and increase ion signal. Instrumental parameters were carefully optimized using cytochrome C and myoglobin to ensure gentle conditions that would facilitate the vaporization and ionization of intact gelsolin 1-3. A quadrupole filter in the ion path was operated in RF only mode, set either to 1430 *m/z* to better transmit ions in the low *m/z* region or 3058 *m/z* for ions in a higher *m/z* region. Transmitted ions entered a collision hexapole where ions were accumulated for 1 sec while being collisionally cooled with argon gas. After the accumulation period, ions were pulsed towards the analyzer cell, which is held at ~10^{-8} mbar, for high resolution mass measurement.

Results and Discussion

SDS-PAGE

The results from the SDS-PAGE experiment in Figure 2 align with what would be expected for gelsolin 1-3. Lane 1 contains the column flow through, i.e. all liquid initially pushed through the column after incubation with the lysed sample. Lanes 2-4 contain washes 1, 2, and 3, respectively. Lane 5 contains the eluent, i.e. the eluted sample, followed by spin-filtered eluent in Lane 6 and the water wash in Lane 7. The spin filtrate, i.e. the liquid filtered from the sample during spin filtration, is in Lane 8, and Lane 9 contains the standard protein ladder.

Lane 1 containing column flow through clearly demonstrates excess soluble cell material and proteins from the sample passing freely through the column. Wash 1 seems to remove most of any leftover material, with a small amount removed by wash 2. By wash 3, all excess material not bound to the column appears to have been removed.

Lanes 5 and 6 are expected to contain the highest concentrations of gelsolin 1-3. The molecular weight of gelsolin 1-3 is approximately 41 kDa, around half that of full-length gelsolin. There is a prominent band just below 49 kDa in these lanes, and while this mass is slightly higher than expected, bands in gels are always approximate masses so some variation is normal. Bands in this range can also be seen in the column flow through and the first wash, indicating either some loss of gelsolin 1-3 or the removal of proteins and cell material with similar molecular weight that did not bind to the column. The gelsolin 1-3 band can also be seen clearly in Lane 7, indicating that some protein remained on

Lotay N., Fortune J Health Sci 2024
DOI:10.26502/fjhs.236

the column, likely due to insufficient incubation time with the elution buffer. The presence of other bands in addition to the strong 49 kDa band in Lanes 5 and 6 demonstrate that the sample is not as pure as would be ideal, likely due to the use of only one purification step. This impurity could also indicate that the slightly higher observed mass is due to some aggregation of smaller protein fragments to the gelsolin 1-3 fragment. While other protocols often call for two or more purification steps, for our purposes of creating a biosensor for the detection of lysophosphatidic acid, the sample does not need to be extremely pure or have a highly accurate concentration, and thus there has not been a need for us to add a second purification method. Finally, the lack of any bands in Lane 8 indicate that no protein was lost during spin filtration.

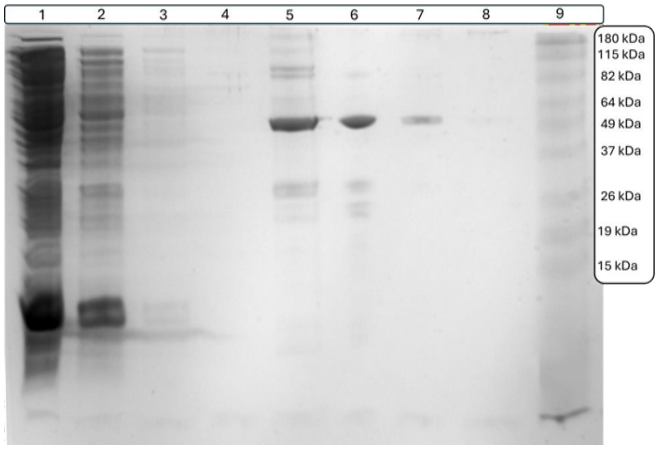

Figure 2: An image of the SDS-PAGE from the synthesis and purification of gelsolin 1-3. The lanes represent samples taken from the different stages of the process: (1) column flow through; (2) wash 1; (3) wash 2; (4) wash 3; (5) eluent; (6) eluent post-spin filtration; (7) water wash; (8) spin filtrate; and (9) Invitrogen™ BenchMark™ Prestained Protein Ladder.

Some of the darker bands observed between 82 and 115 kDa in Lanes 6 and 8 are assumed to be from the gelsolin 1-3 dimerizing with itself, a feature we have observed consistently when conducting this synthesis and purification. As stated previously, the 1- 3 and 4-6 subdomains of gelsolin are homologous, so some dimerization is not only possible but likely and expected. The strong band at 49 kDa in the eluted and dialyzed samples, as well as the dimer bands between 82 and 115 kDa on the ladder, indicate that gelsolin 1-3 was synthesized and purified successfully.

Mass Spectrometry

To further confirm the positive identity of the gelsolin 1-3 protein, it was characterized with mass spectrometry. Mass spectral characterization of the truncated gelsolin protein revealed the presence of multiple distinct species. Initial experiments tuned for a higher *m/z* region showed a predominant species of 33.6 kDa as displayed in Figure 3. The 33.6 kDa mass is lower than the expected 41 kDa for the gelsolin 1-3 sample. A second protein fragment of 68.5 kDa is also present, though at a lower concentration. This species is close to double the mass of the previous fragment, meaning it is most likely formed from dimerization of the 33.6 kDa gelsolin 1-3 fragment. This reinforces the gel electrophoresis results which display a faint band in the 82-115 kDa region in addition to a strong band in the 49 kDa region corresponding with the presence of gelsolin 1-3. As stated above, the 1-3 and 4-6 domains are homologous to each other in the full protein, so dimerization is expected.

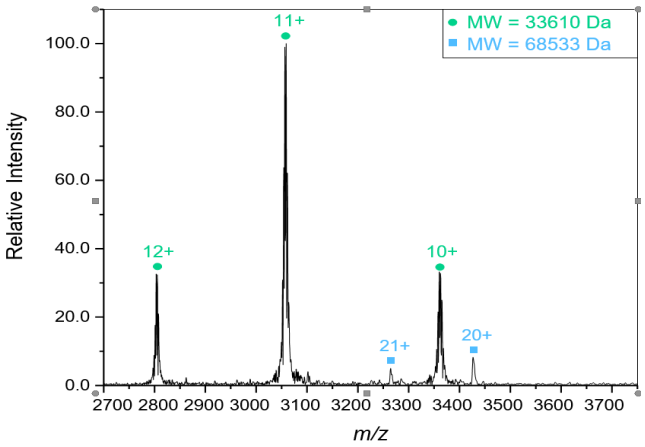

Figure 3: Positive nano-ESI mass spectrum of the sample. In the higher m/z range, a 33.6 kDa molecular weight species is detected predominantly, with charge states indicated on the plot. Lower intensity peaks of a 68.5 kDa species are also present. This latter species is likely to be a dimer of gelsolin 1-3 that resembles the full gelsolin protein.

Since it is possible that a quaternary complex might dissociate upon introduction into the gas phase, the lower *m/z* region was also examined (Figure 4). This revealed the presence of a 14.3 kDa species. The combined masses of the 33.6 kDa and 14.3 kDa species is 47.9 kDa which agrees with the gel electrophoresis results presented in Figure 2. Since gelsolin's individual subdomains are all homologous, it seems that upon introduction to the gas phase, one of the subdomains separated from the other two, giving the 33.6 and 14.3 kDa species seen in the spectrum. It is worth noting that 68.5 kDa and 14.3 kDa is 82.8 kDa, which is approximately equal to the mass of full-length gelsolin or dimerized gelsolin 1-3 (82 kDa). This suggests that the individual subdomain dissociated from the complex upon introduction to the gas phase, especially as it is missing from both the single gelsolin 1-3 and the dimerized gelsolin 1-3. The particular pattern of this dissociation aligning with the masses of gelsolin subdomains also further confirms the identity and presence of gelsolin 1-3.

Lotay N., Fortune J Health Sci 2024
DOI:10.26502/fjhs.236

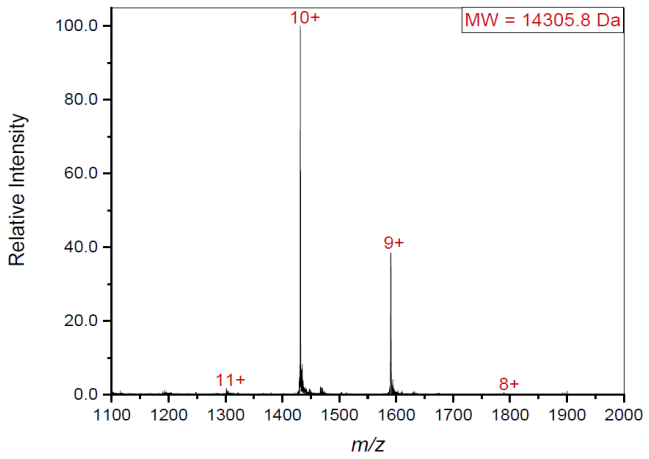

Figure 4: Positive nano-ESI mass spectrum of the sample tuned to the lower m/z range. Multiple charge states of a species with a molecular weight of 14.3 kDa are indicated.

Conclusions

The results from both SDS-PAGE and FTICR-MS of the synthesized sample align to indicate the successful synthesis of gelsolin 1-3. While this has previously been confirmed indirectly by the development of both fluorescence-based and electrochemistry-based biosensors for the detection of lysophosphatidic acid using gelsolin 1-3, this work serves to provide more concrete evidence and structural information about the protein. The total mass was similar to the expected mass of approximately 41 kDa, with small but expected amounts of dimerization being observed. In addition, there was dissociation of a fragment equivalent to the mass of one subdomain from the whole complex, the most likely place for fragmentation to occur. These results combine to support the successful synthesis of gelsolin 1-3, which can now be confidently put to use in future biosensors for the detection of lysophosphatidic acid.

Author Contributions: Conceptualization, N.L, methodology, B.D.L.F., N.L. and C.M.S., validation, N.L. and C.M.S, formal analysis, N.L. and C.M.S, investigation, N.L. and C.M.S, resources, M.T. and R.A.J, writing—original draft preparation, N.L. and C.M.S, writing—review and editing, N.L., C.M.S., B.D.L.F., M.T. and R.A.J, visualization, N.L. and C.M.S, supervision, M.T. and R.A.J, project administration, N.L, funding acquisition, M.T. and R.A.J. All authors have read and agreed to the published version of the manuscript.

Funding: This research was funded by the Canadian Institutes of Health Research (CIHR), grant number PJT 18042 to M.T, the Natural Sciences and Engineering Research Council of Canada (NSERC) Discovery Grant, grant number RG-PIN-2020-05828 to R.A.J, and Canada Foundation for Innovation, grant number 203026 to R.A.J.

Institutional Review Board Statement: Not applicable.

Informed Consent Statement: Not applicable.

Data Availability Statement: The original contributions presented in the study are included in the article; further inquiries can be directed to the corresponding author. The crystal structure depicted in Figure 1 was obtained from RCSB Protein Data Bank under PDB ID: 1RGI; http://doi.org/10.2210/pdb1rgi/pdb.

Acknowledgments

The authors would like to thank Professor Robert C. Robinson of Okayama University for providing the original gelsolin 1-3 plasmids used for this work.

Conflicts of Interest

The authors declare no conflicts of interest. The funders had no role in the design of the study; in the collection, analyses, or interpretation of data; in the writing of the manuscript; or in the decision to publish the results.

References

1. Dominguez R, Holmes KC. Actin Structure and Function. Annual Review of Biophysics 40 (2011): 169–186.
2. Patkowski A. Size, Shape Parameters, and Ca^{2+}-Induced Conformational Change of the Gelsolin Molecule: A Dynamic Light Scattering Study. Biopolymers 30 (3-4): 427–435.
3. Bryan J. Gelsolin Has Three Actin-Binding Sites. Journal of Cell Biology 106 (1988): 1553–1562.
4. Schoepper B, Wegner A. Rate Constants and Equilibrium Constants for Binding of Actin to the 1:1 Gelsolin-Actin Complex. European Journal of Biochemistry 202 (1991): 1127–1131.
5. Gremm D, Wegner A. Co-Operative Binding of Ca^{2+} Ions to the Regulatory Binding Sites of Gelsolin. European Journal of Biochemistry 262 (1999): 330–334.
6. McLaughlin PJ, Gooch JT, Mannherz H-G, Weeds AG. Structure of Gelsolin Segment 1-Actin Complex and the Mechanism of Filament Severing. Nature 364 (1993): 685–692.
7. Nag S, Ma Q, Wang H, Chumnarnsilpa S, Lee WL, Larsson M, et al. Ca^{2+} Binding by Domain 2 Plays a Critical Role in the Activation and Stabilization of Gelsolin. Proceedings of the National Academy of Sciences 106 (2009): 13713-13718.
8. Burtnick LD, Koepf EK, Grimes J, Jones EY, et al. The Crystal Structure of Plasma Gelsolin: Implications for Actin Severing, Capping, and Nucleation. Cell 90 (1997): 661–670.

9. Kwiatkowski DJ, Stossel TP, Orkin SH, Mole JE, et al. Plasma and Cytoplasmic Gelsolins Are Encoded by a Single Gene and Contain a Duplicated Actin-Binding Domain. Nature 323 (1986): 455–458.

10. Burtnick LD, Urosev D, Irobi E, Narayan K, Robinson RC. Structure of the N-Terminal Half of Gelsolin Bound to Actin: Roles in Severing, Apoptosis and FAF. The EMBO Journal 23 (2004): 2713–2722.

11. Goetzl EJ, Lee H, Azuma T, Stossel TP, et al. Gelsolin Binding and Cellular Presentation of Lysophosphatidic Acid. Journal of Biological Chemistry 275 (2000): 14573–14578.

12. Xu Y, Shen Z, Wiper DW, Morton RE, Elson P, Kennedy AW, et al. Lysophosphatidic Acid as a Potential Biomarker for Ovarian and Other Gynecologic Cancers. Journal of the American Medical Association 280 (1998): 719–723.

13. Sedláková I, Vávrová J, Tošner J, Hanousek L. Lysophosphatidic Acid (LPA)-a Perspective Marker in Ovarian Cancer. Tumor Biology 32 (2011): 311–316.

14. SEER*Explorer: An Interactive Website for SEER Cancer Statistics [Internet]. Surveillance Research Program, National Cancer Institute, United States of America; 2024 Apr 17. [updated: 2024 Jun 27].

15. De La Franier B, Thompson M. Detection of the Ovarian Cancer Biomarker Lysophosphatidic Acid in Serum. Biosensors 10 (2020): 13.

16. Ahmadi S, Lotay N, Thompson M. Affinity-Based Electrochemical Biosensor with Antifouling Properties for Detection of Lysophosphatidic Acid, a Promising Early-Stage Ovarian Cancer Biomarker. Bioelectrochemistry 153 (2023): 108466.

17. Davoudian K, Spagnolo S, Lotay N, Satkauskas M, Mészáros G, Hianik T, et al. Design and Characterization of a Dual-Protein Strategy for an Early-Stage Assay of Ovarian Cancer Biomarker Lysophosphatidic Acid. Biosensors 14 (2024): 287.

18. Li H, Nguyen HH, Ogorzalek Loo RR, Campuzano IDG, Loo JA. An Integrated Native Mass Spectrometry and Top-Down Proteomics Method That Connects Sequence to Structure and Function of Macromolecular Complexes. Nature Chemistry 10 (2018): 139–148.

19. Jensen N, Tomer K, Gross M. Fast Atom Bombardment and Tandem Mass Spectrometry of Phosphatidylserine and Phosphatidylcholine. Lipids 21 (1986): 580–588.

20. Rademaker GJ, Heerma W, Haverkamp J. The Fast Atom Bombardment Mass Spectrum and Fragmentation Pathway of N-[2-(Acetamido)-2-Deoxy-β-D-Glucopyranosyl]-L-Asparagine. Biological Mass Spectrometry 21 (1992): 667–671.

21. Hearn JD, Smith GD. A Chemical Ionization Mass Spectrometry Method for the Online Analysis of Organic Aerosols. Analytical Chemistry 76 (2004): 2820–2826.

22. Byrdwell WC. Atmospheric Pressure Chemical Ionization Mass Spectrometry for Analysis of Lipids. Lipids 36 (2001): 327–346.

23. Leney AC, Heck AJR. Native Mass Spectrometry: What Is in the Name? Journal of the American Society for Mass Spectrometry 28 (2017): 5–13.

24. Tamara S, den Boer MA, Heck AJR. High-Resolution Native Mass Spectrometry. Chemical Reviews 122 (2022): 7269–7326.

25. Rose RJ, Labrijn AF, van den Bremer ETJ, Loverix S, Lasters I, et al. Quantitative Analysis of the Interaction Strength and Dynamics of Human IgG4 Half Molecules by Native Mass Spectrometry. Structure 19 (2011): 1274-1282.

26. Pottiez G, Haverland N, Ciborowski P. Mass Spectrometric Characterization of Gelsolin Isoforms. Rapid Communications in Mass Spectrometry 24 (2010): 2620–2624.

27. Sethi S, Dasari S, Amin MS, Vrana JA, Theis JD, et al. Clinical, Biopsy, and Mass Spectrometry Findings of Renal Gelsolin Amyloidosis. Kidney International 91 (2017): 964–971.